Acta Crystallographica Section F
Structural Biology and Crystallization Communications
ISSN 1744-3091

Cloning, expression and crystallization of dihydrodipicolinate reductase from methicillin-resistant *Staphylococcus aureus*

Sudhir Dommaraju,[a]‡ Michael A. Gorman,[b]‡ Con Dogovski,[a] F. Grant Pearce,[c] Juliet A. Gerrard,[c] Renwick C. J. Dobson,[a,c] Michael W. Parker[a,b] and Matthew A. Perugini[a,b]*

[a]Department of Biochemistry and Molecular Biology, Bio21 Molecular Science and Biotechnology Institute, The University of Melbourne, Parkville 3010, Victoria, Australia, [b]St Vincent's Institute of Medical Research, 9 Princes Street, Fitzroy, Victoria 3065, Australia, and [c]School of Biological Sciences, University of Canterbury, Private Bag 4800, Christchurch 8020, New Zealand

‡ These authors contributed equally to this work.

Correspondence e-mail: perugini@unimelb.edu.au

Received 31 August 2009
Accepted 12 November 2009

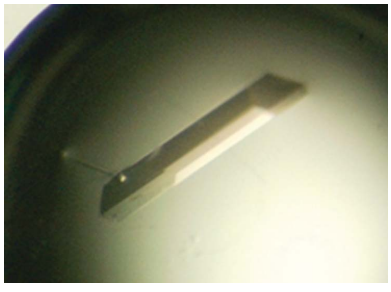

Dihydrodipicolinate reductase (DHDPR; EC 1.3.1.26) catalyzes the nucleotide (NADH/NADPH) dependent second step of the lysine-biosynthesis pathway in bacteria and plants. Here, the cloning, expression, purification, crystallization and preliminary X-ray diffraction analysis of DHDPR from methicillin-resistant *Staphylococcus aureus* (MRSA-DHDPR) are presented. The enzyme was crystallized in a number of forms, predominantly with ammonium sulfate as a precipitant, with the best crystal form diffracting to beyond 3.65 Å resolution. Crystal structures of the apo form as well as of cofactor (NADPH) bound and inhibitor (2,6-pyridinedicarboxylate) bound forms of MRSA-DHDPR will provide insight into the structure and function of this essential enzyme and valid drug target.

1. Introduction

Staphylococcus aureus is a Gram-positive bacterium that is a significant cause of hospital- and community-acquired bacterial infections (Chambers & Deleo, 2009). Emerging antibiotic resistance among most pathogenic bacterial species, including methicillin-resistant *S. aureus* (MRSA), has been a major cause of concern for some time and the focus of widespread scientific and media attention. In order to surmount the threat of microbial drug resistance, there is an urgent need to develop new drugs, preferably with a new mode of action, and a consequent need to characterize novel drug targets (Hutton *et al.*, 2003). One target that has yet to be exploited is the lysine-biosynthesis pathway (Hutton *et al.*, 2007). This pathway yields lysine and *meso*-diaminopimelate, which are vital constituents of the bacterial peptidoglycan cell wall in Gram-positive bacteria and in Gram-negative bacteria, respectively (Hutton *et al.*, 2007). Hence, inhibitors of the lysine-biosynthetic pathway may provide a new class of antibacterial agents that act by inhibiting cell wall and/or protein synthesis. This is a priority pathway to target, given that mammals lack the ability to synthesize lysine *de novo* and therefore must acquire this essential amino acid from dietary sources. The occurrence of the lysine-biosynthetic pathway in microorganisms but not in mammals suggests that specific inhibitors of the enzymes involved in bacterial lysine biosynthesis may display novel antibacterial activity with low mammalian toxicity. One such enzyme is the product of the essential *dapB* gene (Kobayashi *et al.*, 2003): dihydrodipicolinate reductase (DHDPR). DHDPR catalyzes the second step in the pathway, namely the pyridine nucleotide-dependent reduction of dihydrodipicolinate (DHDP) to form tetrahydrodipicolinic acid (THDP) (Tamir & Gilvarg, 1974).

The three-dimensional structures of DHDPR from *Escherichia coli* (Reddy *et al.*, 1996; Scapin *et al.*, 1995, 1997) and *Mycobacterium tuberculosis* (Cirilli *et al.*, 2003) have been elucidated by X-ray crystallography. DHDPR assembles as a tetrameric enzyme made up of identical subunits, with each monomer comprising of an N-terminal nucleotide-binding domain and a C-terminal substrate-binding domain (Scapin *et al.*, 1995, 1997). Cofactor (NADPH) bound and the inhibitor 2,6-pyridinedicarboxylate (2,6-PDC) bound structures of DHDPR from *E. coli* and *M. tuberculosis* have enabled identification of the residues involved in catalysis (Scapin *et al.*, 1997; Cirilli *et al.*, 2003). The crystal structure of DHDPR from *Thermatoga maritima*

(PDB code 1vm6; Joint Center for Structural Genomics, unpublished work) and the more recently added polymorphic forms of DHDPR from *M. tuberculosis* (PDB codes 1yl5, 1yl6 and 1yl7; Janowski *et al.*, 2010) have furthered the understanding of this essential enzyme. In this study, we describe the cloning, expression, purification, crystallization and preliminary X-ray diffraction data of DHDPR from the pathogen MRSA.

2. Methods and materials

2.1. Gene cloning

The *dapB* gene and flanking nucleotide sequence was amplified by PCR from the genomic DNA of MRSA252 using the primer pair OSD1 (CAT TGG TTA GCC TAG AAG ATA C) and OSD2 (TCT GGA TAT GTG ATG CCT TC). The resulting PCR product was cloned into the pCRBlunt II-TOPO (Invitrogen) vector to create pDD002. *Nde*I and *Bam*HI restriction sites were incorporated into the 5′ and 3′ ends of the *dapB* gene by PCR using the primer pair OSD3 (CAT ATG AAA ATA TTA CTA ATT GGC) and OSD4 (ATC CTT ATA GGT TGT CAA ACG TA), respectively. The resulting PCR product was digested with the restriction enzymes *Nde*I and *Bam*HI and subsequently cloned into the corresponding sites of the pET11a expression vector (New England Biolabs) to produce pDD003. The identity of the MRSA *dapB* gene was verified by restriction analysis and dideoxynucleotide sequencing.

2.2. Expression and purification

Expression of recombinant MRSA-DHDPR was conducted using a similar protocol to that described previously for another enzyme in the lysine biosynthesis pathway (Dobson *et al.*, 2008). An overnight pre-culture of transformed BL21 (DE3) cells was used to inoculate 1 l Luria Broth containing 50 µg ml^{-1} ampicillin. The culture was then grown at 310 K to an OD_{600} of 0.7 and treated with 1.0 m*M* isopropyl β-D-1-thiogalactopyranoside to induce recombinant protein expression. Cells were harvested 3 h post-induction by centrifugation at 8000*g* for 20 min. The resultant cell pellets were resuspended in 20 m*M* Tris–HCl pH 8.0 (buffer *A*) and subjected to cell lysis by sonication with an MSE Soniprep 150 sonicator at 10 µm amplitude (20 s bursts followed by a 40 s rest period for a total of 10 min). The cell lysate was clarified by centrifugation at 7000*g* followed by passage through a 5 µm syringe filter (Millipore). The purification of MRSA-DHDPR involved a three-step strategy which included ion-exchange (Q-Sepharose), hydrophobic interaction (Phenyl-Sepharose) and size-exclusion (Superose 12) liquid chromatography. The filtered supernatant was loaded onto an XK 30/50 column (GE Healthcare) containing 25 ml Q-Sepharose fast-flow resin pre-equilibrated with buffer *A* and washed with the same buffer until a stable baseline was established. Elution was performed over five column volumes (CV) in the same buffer employing a gradient of 0–1.0 *M* NaCl. The enzyme typically eluted between 0.4 and 0.6 *M* NaCl and the fractions corresponding to DHDPR were pooled and dialysed in 30 m*M* Tris–HCl, 1.0 *M* NaCl, pH 8.0 (buffer *B*) before proceeding to the second step of purification. The dialysed protein was then applied onto another XK 30/50 column (GE Healthcare) containing 25 ml Phenyl Sepharose fast-flow resin pre-equilibrated with buffer *B*. Greater than 95% pure recombinant product eluted unbound from the column, whilst the other impurities bound to it. The unbound fraction containing >95% pure recombinant MRSA-DHDPR was then dialysed against 20 m*M* Tris–HCl pH 8.0 and concentrated to 10 mg ml^{-1} using an Amicon concentrator (molecular-weight cutoff 10 000 Da) before being pooled and aliquoted. Each 500 µl aliquot was then loaded onto a pre-packed Superose 12 10/300 gel-filtration column pre-equilibrated with 20 m*M* Tris–HCl, 150 m*M* NaCl, pH 8.0 for further use.

2.3. Electrospray ionization mass spectrometry

Electrospray ionization time-of-flight (ESI-TOF) mass spectrometry was performed on the recombinant protein sample in 20 m*M* Tris–HCl and 150 m*M* NaCl pH 8.0 to confirm the molecular weight

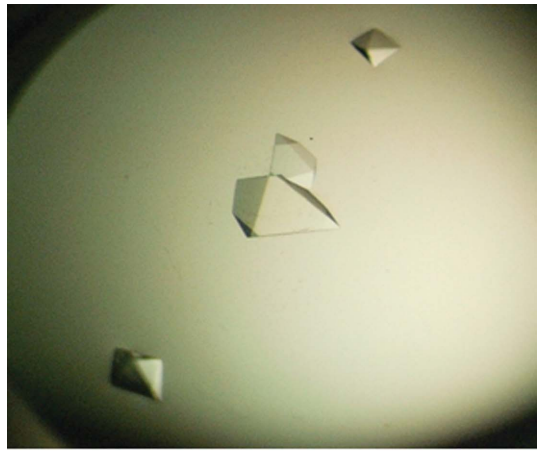

(*a*)

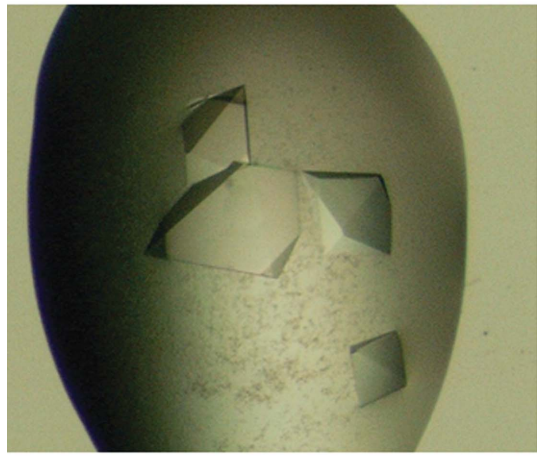

(*b*)

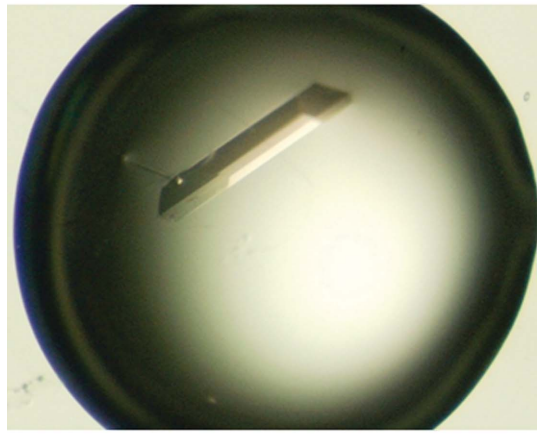

(*c*)

Figure 1
Crystals of (*a*) apo MRSA-DHDPR, (*b*) MRSA-DHDPR in the presence of NADPH cofactor and (*c*) MRSA-DHDPR in the presence of NADPH and the substrate analogue 2,6-PDC.

Table 1
Purification of MRSA-DHDPR.

Fraction	Protein (mg)	Total activity (U)	Specific activity (U mg^{-1})	Purification factor (fold)
Crude	542	930	1.70	1.0
Q-Sepharose	233	1180	5.10	3.0
Phenyl Sepharose	112	662	5.90	3.4
Superose 12	44.2	481	10.1	5.9

of the recombinant protein. The sample in acetonitrile/0.04%(*v*/*v*) formic acid was injected directly into a 6210 LC/MS ESI-TOF (Agilent Technologies). Data were analyzed using the program *Mass Hunter* (Agilent Technologies).

2.4. Protein crystallization

The crystallization of MRSA-DHDPR was performed as described previously (Atkinson *et al.*, 2009; Burgess, Dobson, Dogovski *et al.*, 2008; Dobson *et al.*, 2008; Voss *et al.*, 2009). Recombinant enzyme (9.0 mg ml^{-1}) solubilized in 20 m*M* Tris–HCl, 150 m*M* NaCl at pH 8.0 was subjected to initial crystallization trials at the CSIRO node of the Bio21 Collaborative Crystallization Centre (C3; http://www.csiro.au/c3/) using Qiagen PACT Suite and JCSG+ Suite crystal screens. Ammonium Sulfate Suite (Qiagen) crystal screens at 281 and 293 K were also conducted. These initial screens were set up in 96-well plates using the sitting-drop vapour-diffusion method with droplets consisting of 100 nl protein solution and 100 nl reservoir solution. Several crystal forms were obtained at both temperatures after 3 d under varying conditions. Selected conditions were chosen from the initial C3 screens and larger-scale crystal screens were set up in-house in 24-well Linbro plates (Hampton Research) using the hanging-drop vapour-diffusion method at 293 K. These screens were predominantly comprised of reservoir conditions containing ammonium sulfate as the precipitant in the presence of sodium halides, such as NaF and NaBr, at pH 6.5–8.0. The crystal form shown in Fig. 1(*a*) was obtained from a 2 µl drop made up of 1 µl protein solution (9.2 mg ml^{-1} in 20 m*M* Tris–HCl, 150 m*M* NaCl pH 8.0) and 1 µl reservoir buffer (2.4 *M* ammonium sulfate, 0.2 *M* sodium fluoride and 0.1 *M* bis-tris propane pH 7.5) and incubated at 281 K. The crystal forms shown in Fig. 1(*b*) were obtained under similar conditions, but the protein was pre-incubated with 10 m*M* NADPH on ice for 30 min before the drops were set up. The best diffracting crystals (Fig. 1*c*) were obtained by the addition of 10 m*M* 2,6-PDC and 10 m*M* NADPH to the protein solution. Ethanol to a final concentration of 10%(*v*/*v*) was then added to the reservoir.

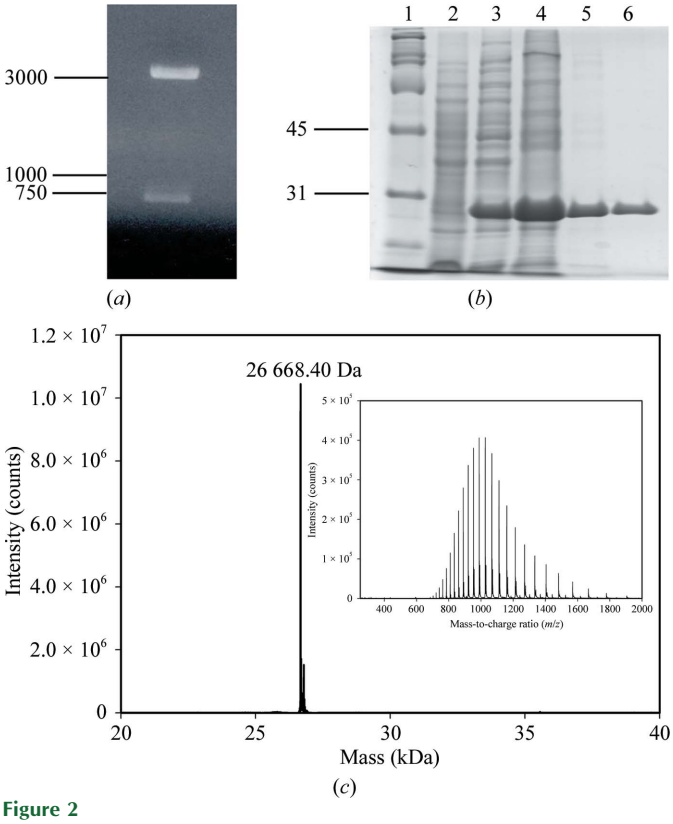

Figure 2
(*a*) Agarose-gel analysis following *Nde*I and *Bam*HI restriction-endonuclease digestion of the plasmid pDD003, depicting the cut pET11a vector and the *dapB* gene. Markers are labelled in base pairs. (*b*) SDS–PAGE gel showing the expression and purification of MRSA-DHDPR. Lane 1, molecular-weight markers (kDa); lane 2, *E. coli* BL21 (DE3) cell-free extract; lane 3, extract after induction with 1 m*M* IPTG for 3 h; lane 4, pooled Q-Sepharose fractions; lane 5, pooled Phenyl Sepharose fractions; lane 6, pooled Superose 12 fractions. (*c*) Deconvoluted ESI-TOF mass spectrum of MRSA-DHDPR showing a major peak with mass of 26 668.40 Da, which is consistent with the theoretical monomer mass of the enzyme. Inset: raw MS data plotted as intensity *versus* mass-to-charge ratio.

Table 2
X-ray data-collection statistics.

Values in parentheses are for the highest resolution shell.

Temperature (K)	100
No. of crystals	1
Crystal-to-detector distance (mm)	421.85
Oscillation angle per frame (°)	0.5
Wavelength (Å)	0.95663
Unit-cell parameters (Å)	$a = b = 90.4$, $c = 524.0$
Resolution (Å)	50.0–3.65 (3.87–3.65)
No. of observations	278533
Multiplicity	17.67 (4.93)
No. of unique reflections	14734
Refined mosaicity (°)	0.217
Completeness (%)	96.1 (77.6)
Mean $I/\sigma(I)$	21.91 (7.94)
$R_{\rm merge}$† (%)	4.5 (12.0)
$R_{\rm meas}$‡ (%)	11.8 (21.2)
Wilson *B* factor (Å^2)	32.3

† $R_{\rm merge} = 100 \times \sum_{hkl} \sum_i |I_i(hkl) - \langle I(hkl)\rangle| / \sum_{hkl} \sum_i I_i(hkl)$, where $I_i(hkl)$ is the *i*th measurement of the intensity of reflection *hkl* and $\langle I(hkl)\rangle$ is its mean value. ‡ $R_{\rm meas}$ is the redundancy-independent merging *R* factor (Diederichs & Karplus, 1997). $R_{\rm meas} = 100 \times \sum_{hkl}[N/(N-1)]^{1/2} \sum_i |I_i(hkl) - \langle I(hkl)\rangle| / \sum_{hkl} \sum_i I_i(hkl)$, where *N* is the number of times a given reflection has been observed.

2.4.1. Data collection and processing. Diffraction data were collected for all three crystal forms using the MX1 beamline at the Australian Synchrotron, Clayton. Intensity data were collected at 100 K on an ADSC Q210r detector. A 220.5° data set was collected from the crystal shown in Fig. 1(*c*), with an oscillation angle of 0.5° and an exposure time of 5 s per diffraction image. Processing and scaling of the data was carried out using the program *XDS* (Kabsch, 1993).

3. Results and discussion

The *dapB* gene encoding MRSA-DHDPR was successfully cloned into the pET11a expression vector (Fig. 2*a*) and the resultant plasmid pDD003 was transformed into *E. coli* BL21 (DE3) cells for over-expression of the recombinant enzyme. The purity of the recombinant MRSA-DHDPR after the three-step liquid-chromatography strategy was estimated by SDS–PAGE to be >95% (Fig. 2*b*). This was confirmed by ESI-TOF mass spectrometry, which showed that the recombinant enzyme had a molecular mass of 26 668 Da, which was consistent with the theoretical mass of the MRSA-DHDPR monomer of 26 668.40 Da (Fig. 2*c*). MRSA-DHDPR was also demonstrated to be enzymatically active using a coupled assay (Burgess, Dobson, Bailey *et al.*, 2008; Dobson *et al.*, 2004; Griffin *et al.*, 2008). The

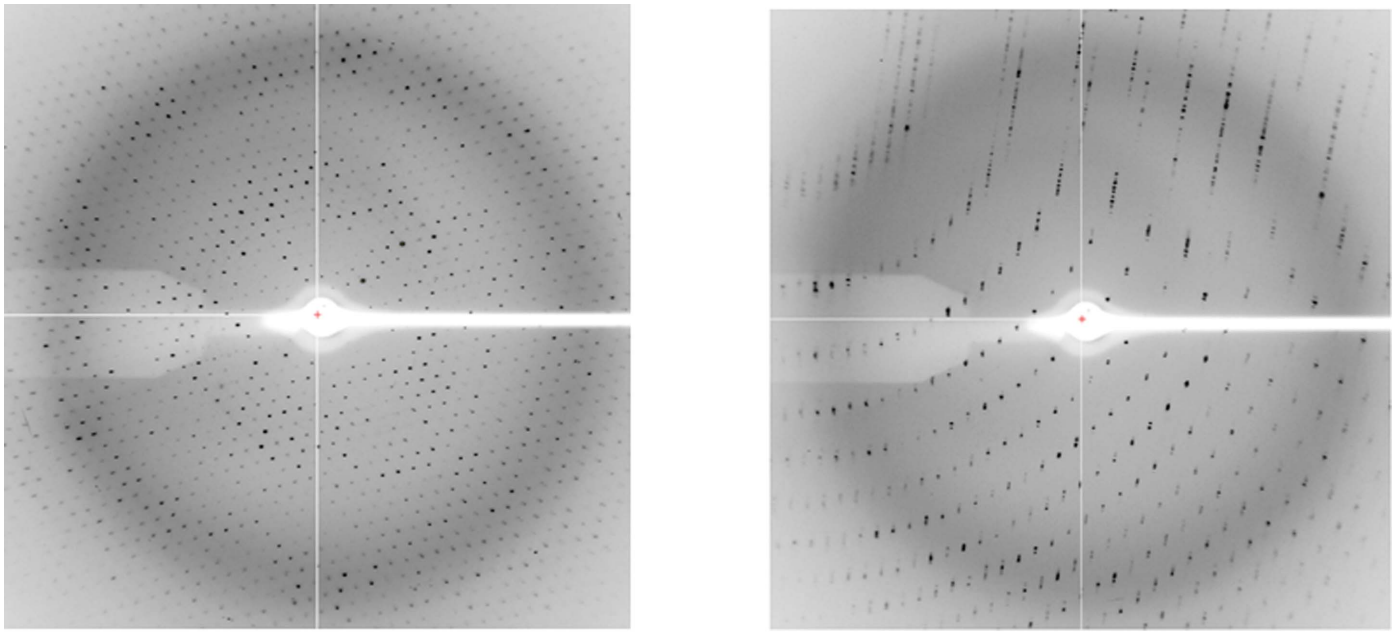

(*a*) (*b*)

Figure 3
X-ray diffraction frames from crystals of MRSA-DHDPR co-crystallized with NADPH and 2,6-PDC.

purified enzyme has a specific activity of 10.1 U mg^{-1}, with an overall purification of 5.9-fold (Table 1). Purified recombinant MRSA-DHDPR was subjected to crystallization trials.

MRSA-DHDPR crystallized under identical conditions in the presence and absence of cofactor (NADPH). The diffraction from both crystal forms (Figs. 1*a* and 1*b*) was of poor quality and data were therefore not collected. However, addition of the substrate analogue 2,6-PDC to the cofactor-bound protein, as well as of ethanol as an additive to the reservoir buffer, resulted in a different crystal form (Fig. 1*c*) which diffracted to at least 3.6 Å resolution (Figs. 3*a* and 3*b*). The crystals diffracted to a higher resolution but owing to the long cell dimensions and small detector area we were unable to collect the highest resolution data possible. Preliminary analysis of the X-ray diffraction data (Figs. 3*a* and 3*b*) indicated that the unit-cell parameters of the crystal shown in Fig. 1(*c*) were a = 90.4, b = 90.4, c = 524.0 Å (Table 2). This suggested that the crystal belonged to a hexagonal crystal system. Complete data-collection statistics are shown in Table 2. We are currently optimizing the crystallization conditions and will be collecting further data using an ADSC Q315r detector in order to obtain higher resolution data. We anticipate that the structure of MRSA-DHDPR will provide insight into the design of novel antimicrobials.

We would firstly like to acknowledge Associate Professor Geoff Hogg from the Microbiological Diagnostic Unit, University of Melbourne, Public Health Laboratory Network, Department of Health and Ageing, Australia for providing genomic DNA from a clinical isolate of MRSA252. We would also like to acknowledge the support and assistance of the friendly staff, particularly Dr Janet Newman, at the Bio21 Collaborative Crystallographic Centre at CSIRO Molecular and Health Technologies, Parkville, Melbourne as well as all members of the Perugini laboratory for helpful discussions during the preparation of this manuscript. This research was undertaken on the MX1 beamline at the Australian Synchrotron, Victoria, Australia. The views expressed herein are those of the authors and are not necessarily those of the owner or operator of the Australian Synchrotron. Finally, we acknowledge the Defense Threat Reduction Agency (DTRA; Project ID AB07CBT004) for program funding and the Australian Research Council for providing a Future Fellowship to MAP and a Federation Fellowship to MWP. RCJD acknowledges the C. R. Roper bequest for salary support.

References

Atkinson, S. C., Dobson, R. C. J., Newman, J. M., Gorman, M. A., Dogovski, C., Parker, M. W. & Perugini, M. A. (2009). *Acta Cryst.* F**65**, 253–255.
Burgess, B. R., Dobson, R. C. J., Bailey, M. F., Atkinson, S. C., Griffin, M. D. W., Jameson, G. B., Parker, M. W., Gerrard, J. A. & Perugini, M. A. (2008). *J. Biol. Chem.* **283,** 27598–27603.
Burgess, B. R., Dobson, R. C. J., Dogovski, C., Jameson, G. B., Parker, M. W. & Perugini, M. A. (2008). *Acta Cryst.* F**64**, 659–661.
Chambers, H. F. & Deleo, F. R. (2009). *Nature Rev. Microbiol.* **7**, 629–641.
Cirilli, M., Zheng, R., Scapin, G. & Blanchard, J. S. (2003). *Biochemistry*, **42**, 10644–10650.
Diederichs, K. & Karplus, P. A. (1997). *Nature Struct. Biol.* **4**, 269–275.
Dobson, R. C. J., Atkinson, S. C., Gorman, M. A., Newman, J. M., Parker, M. W. & Perugini, M. A. (2008). *Acta Cryst.* F**64**, 206–208.
Dobson, R. C. J., Valegård, K. & Gerrard, J. A. (2004). *J. Mol. Biol.* **338**, 329–339.
Griffin, M. D. W., Dobson, R. C. J., Pearce, F. G., Antonio, L., Whitten, A. E., Liew, C. K., Mackay, J. P., Trewhella, J., Jameson, G. B., Perugini, M. A. & Gerrard, J. A. (2008). *J. Mol. Biol.* **380**, 691–703.
Hutton, C. A., Perugini, M. A. & Gerrard, J. A. (2007). *Mol. Biosyst.* **3**, 458–465.
Hutton, C. A., Southwood, T. J. & Turner, J. J. (2003). *Mini Rev. Med. Chem.* **3**, 115–127.
Janowski, R., Kefala, G. & Weiss, M. S. (2010). *Acta Cryst.* D**66**, 61–72.
Kabsch, W. (1993). *J. Appl. Cryst.* **26**, 795–800.
Kobayashi, K. *et al.* (2003). *Proc. Natl Acad. Sci. USA*, **100**, 4678–4683.
Reddy, S. G., Scapin, G. & Blanchard, J. S. (1996). *Biochemistry*, **35**, 13294–13302.
Scapin, G., Blanchard, J. S. & Sacchettini, J. C. (1995). *Biochemistry*, **34**, 3502–3512.
Scapin, G., Reddy, S. G., Zheng, R. & Blanchard, J. S. (1997). *Biochemistry*, **36**, 15081–15088.
Tamir, H. & Gilvarg, C. (1974). *J. Biol. Chem.* **249**, 3034–3040.
Voss, J. E., Scally, S. W., Taylor, N. L., Dogovski, C., Alderton, M. R., Hutton, C. A., Gerrard, J. A., Parker, M. W., Dobson, R. C. J. & Perugini, M. A. (2009). *Acta Cryst.* F**65**, 188–191.